## Extended data figures and tables

**Table 1:** Variables Used to Predict Particle Size Distribution Parameters, Dimensions used and Data Sources

| Feature category | Feature | Dimensions | Sources |
|---|---|---|---|
| Universal | Temperature | 360x180x67x12 | WOA 18[7] |
| | Salinity | 360x180x67x12 | WOA 18[32] |
| | Silicate | 360x180x67x12 | WOA 18[33] |
| | Depth | 360x180x67x12 | WOA 18[7] |
| | Shortwave radiation | 360x180x12 | ERA 5[34] |
| Oxygen | Oxygen | 360x180x67x12 | WOA 18[35] |
| | AOU | 360x180x67x12 | WOA 18[35] |
| Nutrients | Nitrate | 360x180x67x12 | WOA 18[33] |
| | Phosphate | 360x180x67x12 | WOA 18[33] |
| CHL | Merged Chlorophyll | 360x180x12 | GlobColour[36]4/16/25 9:50:00 AM |
| | Modis Chlorophyll | 360x180x12 | NASA G.S.F.C[37] |
| MLD | Mixed layer depth | 360x180x12 | MIMOC[38] |
| | Mixed Layer Depth | 360x180x12 | de Boyer Montégut et al. (2004)[39]4/16/25 9:50:00 AM |
| NPP | Eppley VGPM | 360x180x12 | Antoine and Morel (1996) [40] |
| | VGPM | 360x180x12 | Behrenfeld and Falkowski (1997)[41] |
| | CBPM | 360x180x12 | Westberry et al. (2008)[42] |
| | CAFE | 360x180x12 | Silsbe et al. (2016)[43] |
| Euphotic Depth | Eppley VGPM Euphotic depth | 360x180x12 | Morel et al. (2007)[44] |

| | | | |
|---|---|---|---|
| | VGPM Euphotic depth | 360x180x12 | Morel et al. (2007)[44] |
| | CBPM Euphotic depth | 360x180x12 | Morel et al. (2007)[44] |
| Iron deposition | Labile fraction | 360x180x12 | Myriokefalitakis et al. (2018)[45] |
| | Soluble Fraction | 360x180x12 | Hamilton et al. (2019)[46] |

**Table 2:** Summary table of optimizations for fitting the two-component biological pump.

| Parameter / metric | Meaning | Unit | Southern | Subtropics | Tropics | Subpolar | Global |
|---|---|---|---|---|---|---|---|
| $R_{mig}$ | Ratio of migrant to gravitational export | unitless | 0.18 | 0.11 | 0.18 | 0.13 | 0.16 |
| $b_{grav}$ | Martin exponent for gravitational pump | unitless | 1.04 | 1.67 | 1.53 | 1.09 | 1.4 |
| $b_{mig}$ | Martin exponent for migrant pump | unitless | 0.45 | 0.50 | 0.61 | 0.65 | 0.52 |
| $z_{mig}$ | Central depth of migrant pump particle injection | m | 426 | 387 | 350 | 390 | 344 |
| $H_{mig}$ | Gaussian width for migrant pump particle injection | m | 135 | 98 | 109 | 105 | 109 |
| r2-statistic | Model-data fit | unitless | 0.99 | 0.98 | 0.98 | 0.99 | 0.99 |

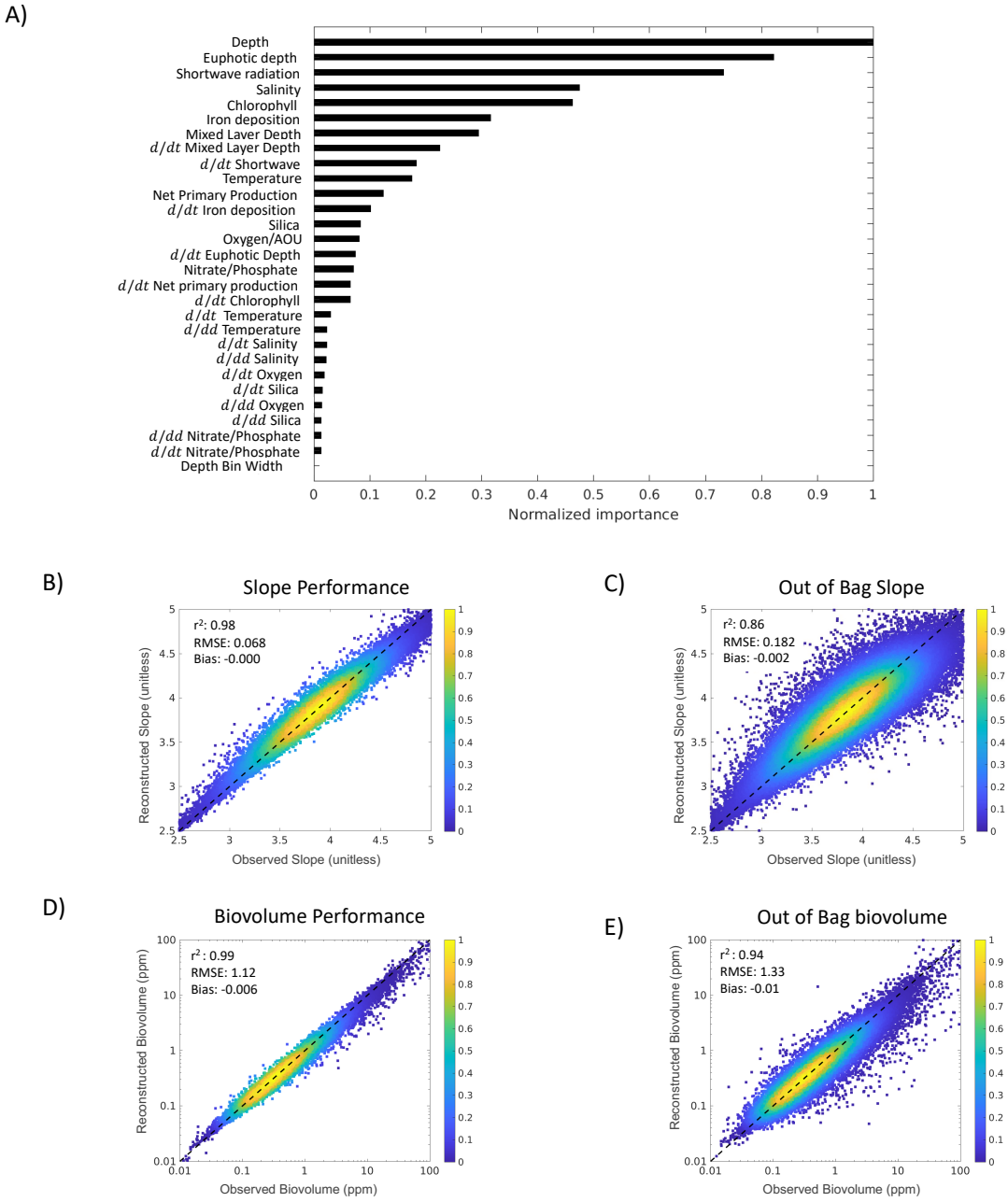


**Figure 1**: (A) Recursive feature elimination results, showing the rank of predictor importance. (B, D) Performance of the Random Forest reconstruction, shown as density scatter plots of predicted versus observed slope ($\beta$) and biovolume (BV), where colors indicate the normalized density of observations at each point. (C, E) same as panel (B, D), but using out-of-bag (OOB) reconstructions, that is, reconstructions vs. observations withheld from training. Annotations in each panel show the coefficient of determination ($r^2$), the root mean square error (RMSE), and the global mean bias.

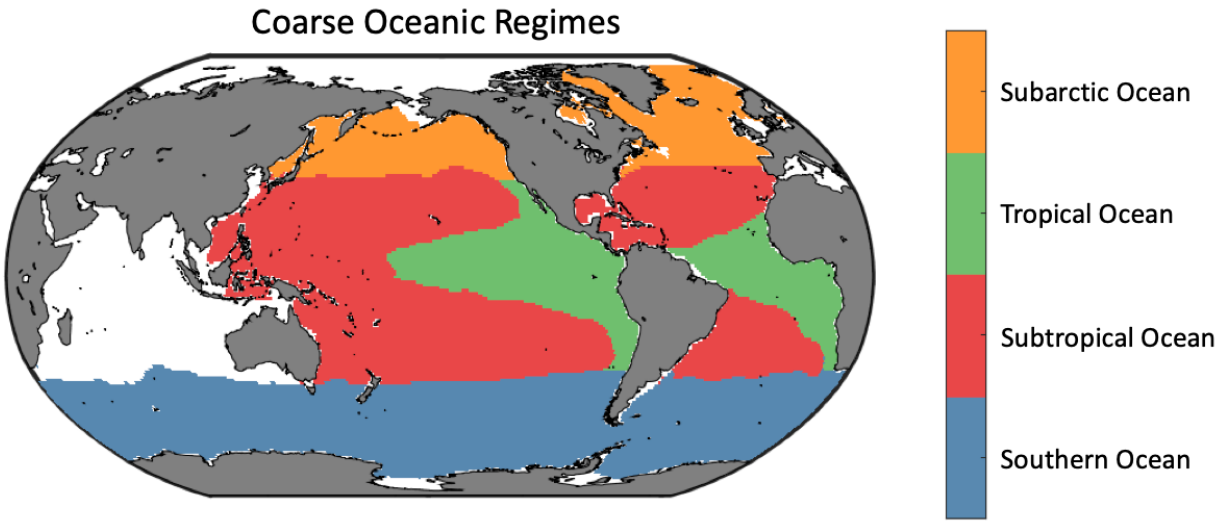


**Figure 2**: Coarse oceanic regions[47] used to calculate the global mean profiles shown in Figures 1-2; using the same color coding.

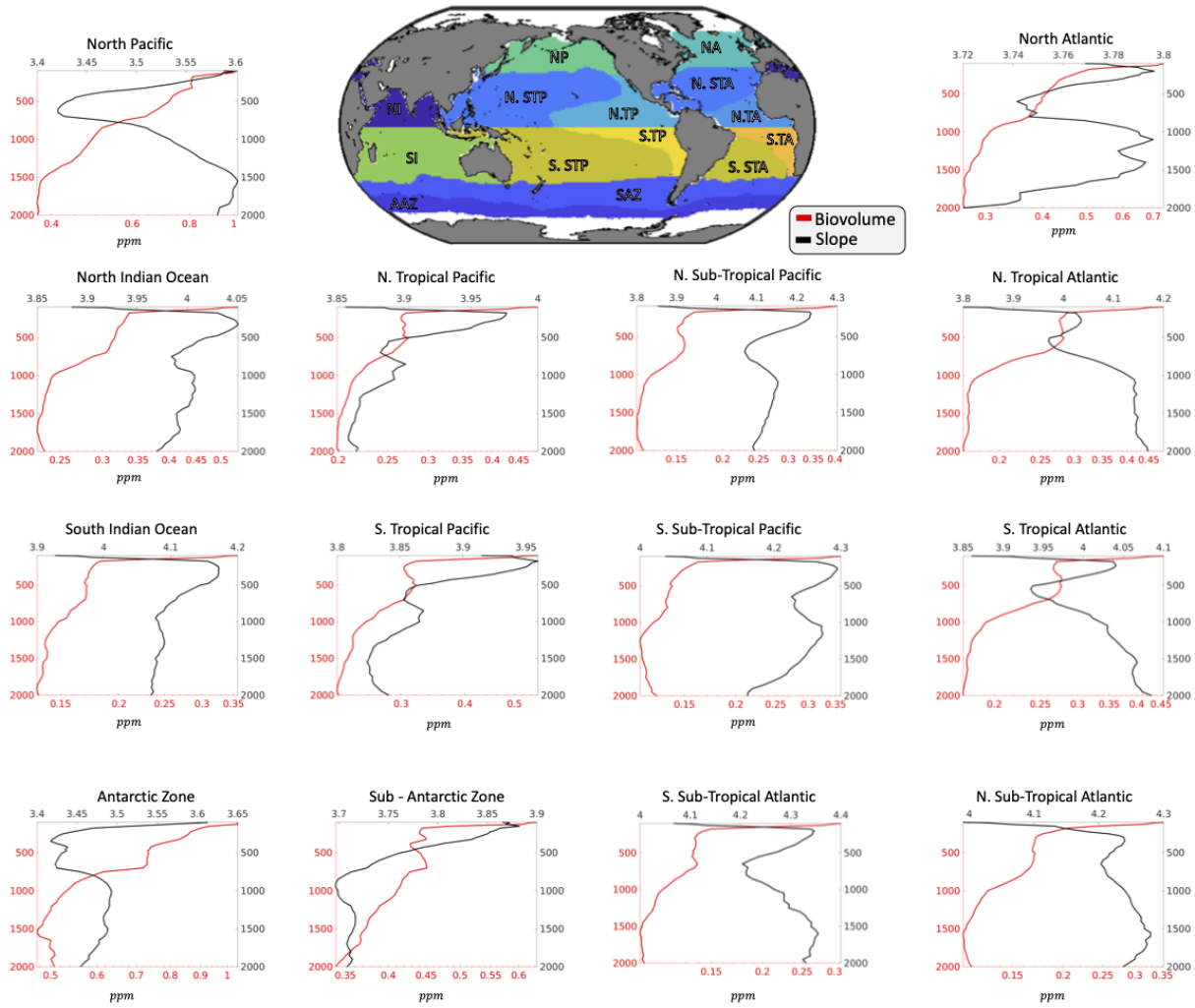


**Figure 3**: Regional mean depth sections for the PSD biovolume (red) and slope (black) for the different sub-regions shown in the map.

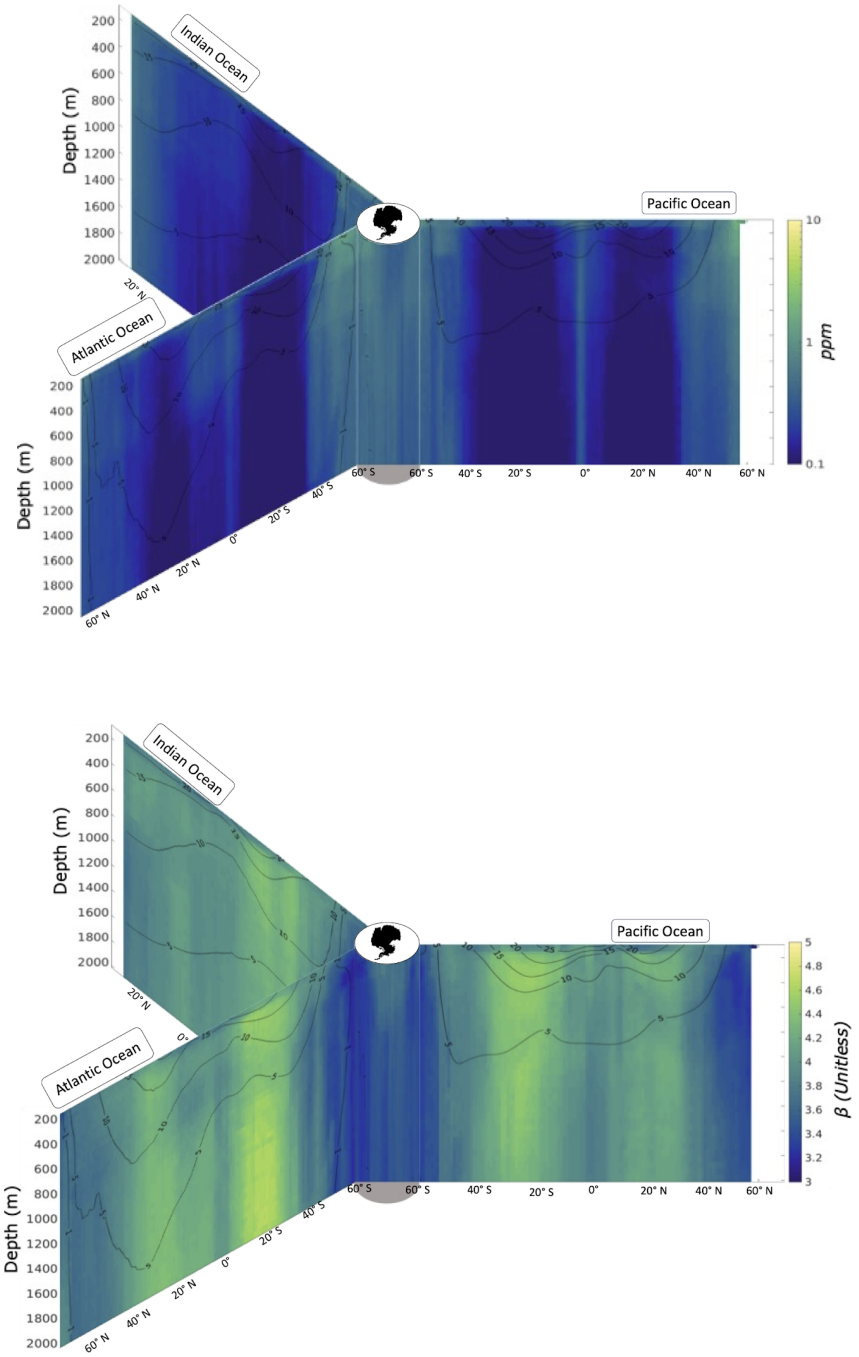


**Figure 4:** Reconstructed depth sections of (A) PSD biovolume and (B) slope for the three major ocean basins. Solid black contours show isotherms at 5 °C intervals. Sections are shown along 155ºW in the Pacific, 25ºW in the Atlantic, and 63ºE in the Indian Ocean.

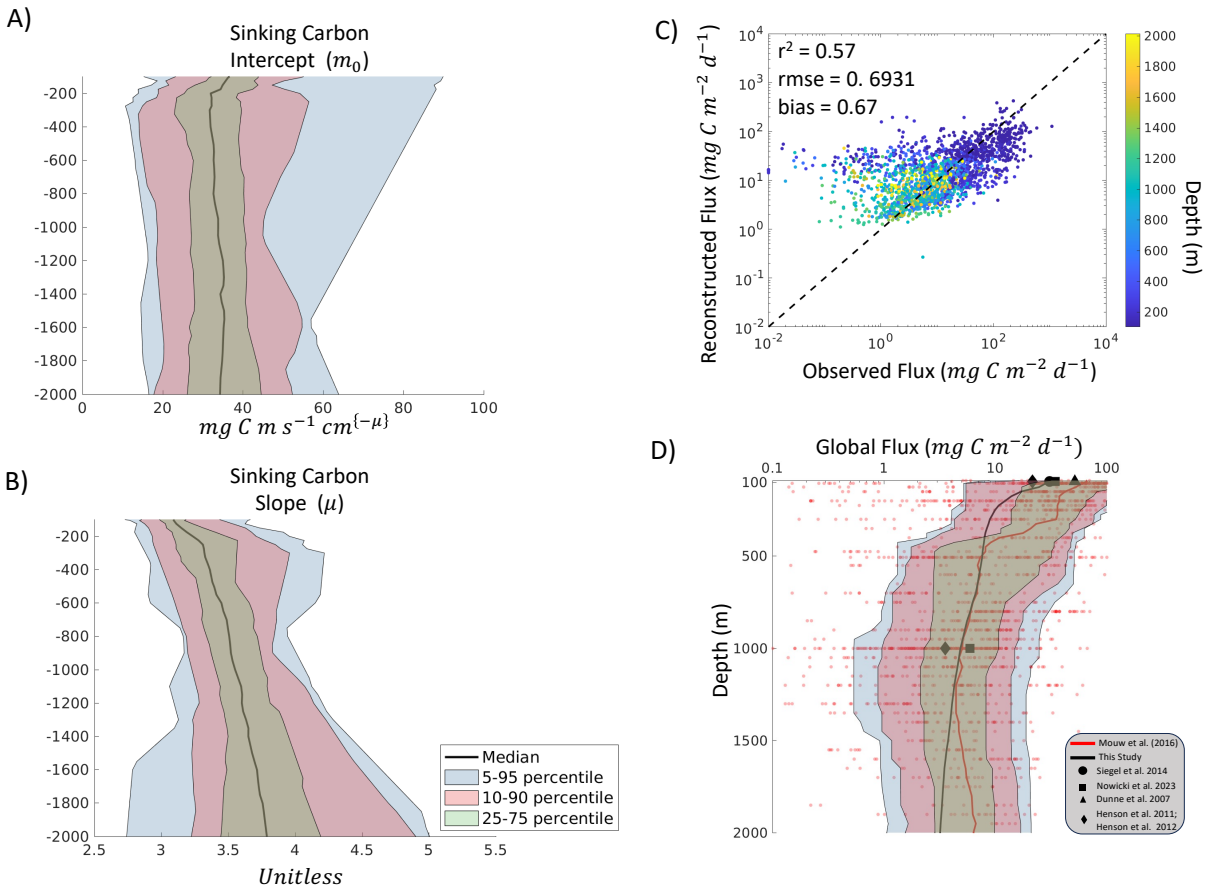


**Figure 5**: Optimized profiles of the global mean sinking carbon parameters $m_0$ and $\mu$ in Equation 7, and the resulting mean global profile of carbon export. Shadings show ranges from 50 independent optimizations with variable shapes of the profiles of $m_0$ and $\mu$.

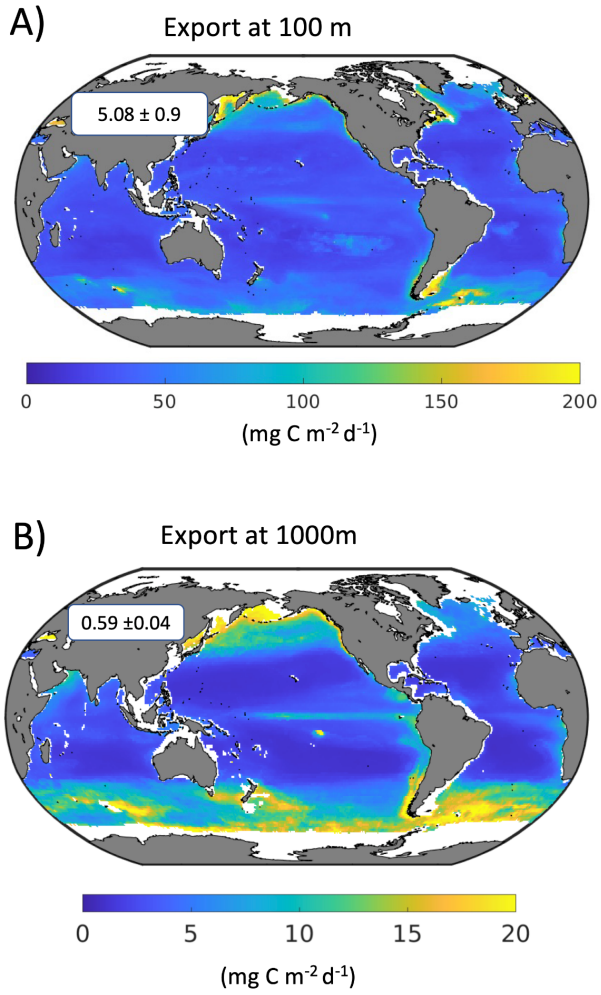


**Figure 6**: Reconstructed annual mean sinking POC flux at the surface (100 m; A), and at the base of the mesopelagic zone (1000 m; B). Annotations show the globally integrated annual sinking POC flux in Pg C/yr.

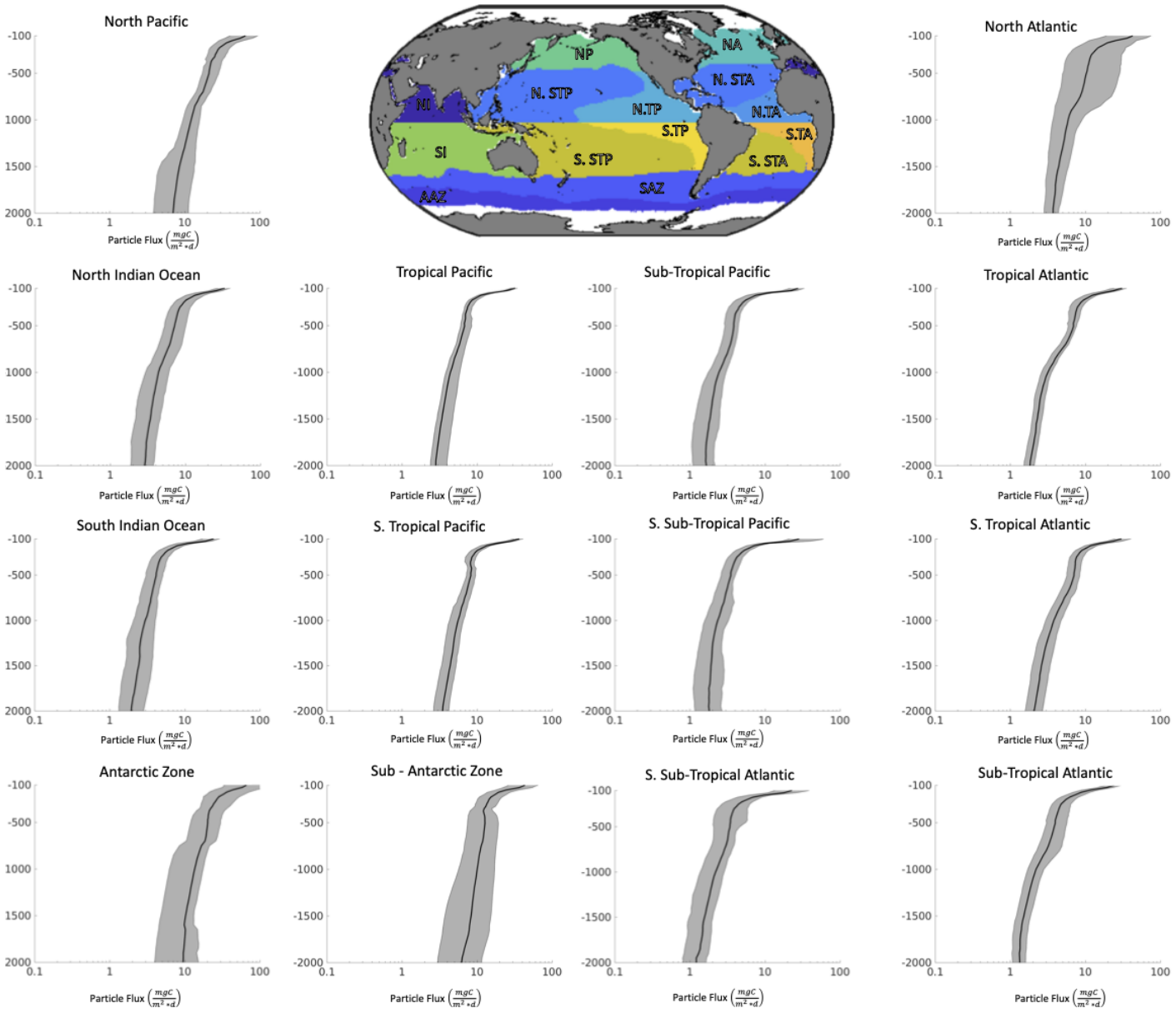


**Figure 7**: Regional mean depth sections for the POC flux (solid black line), with the seasonal cycle (gray shading) for the different sub-regions shown in the map.

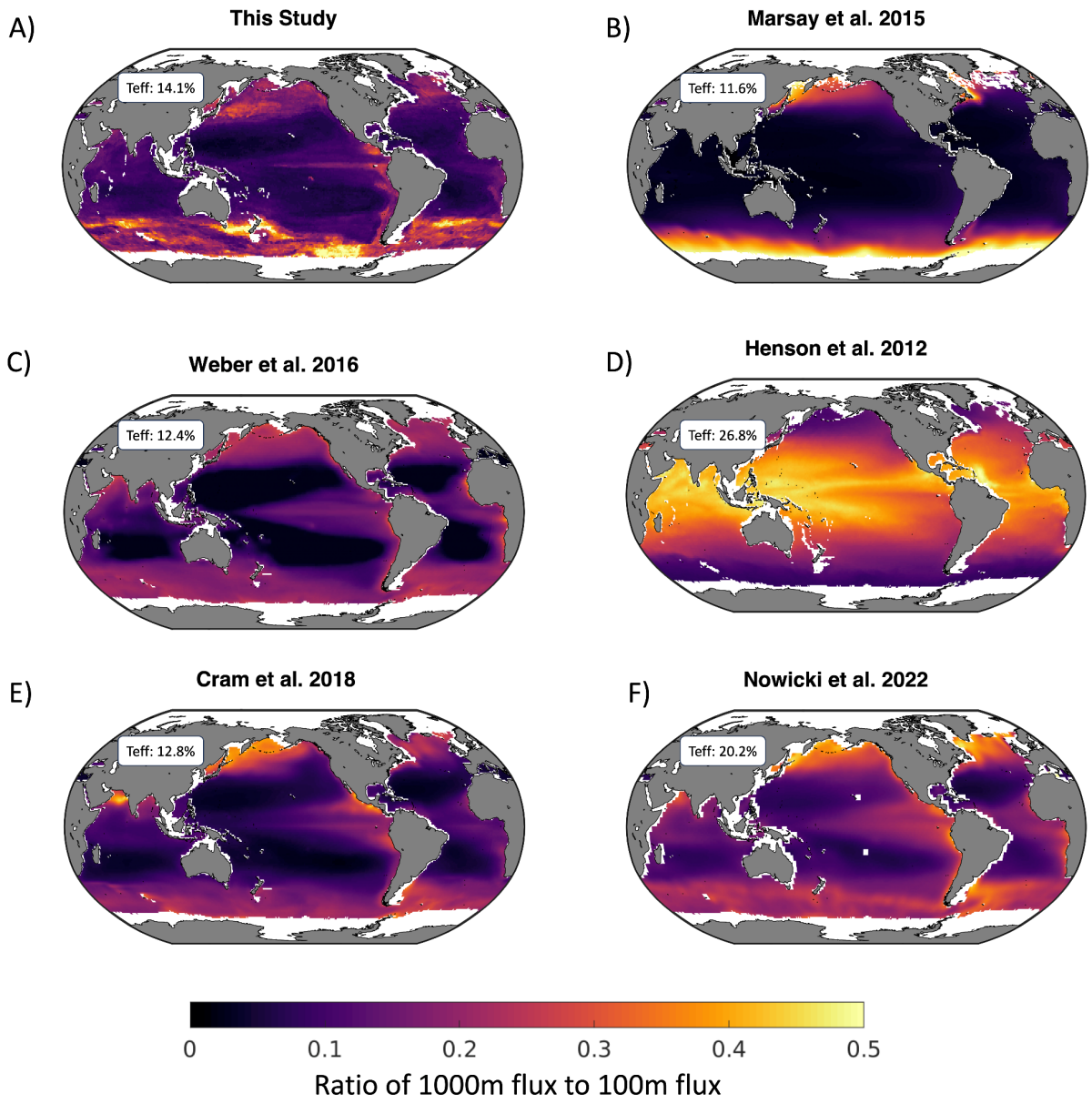


**Figure 8**: Comparison of our results (A, see also Fig. 3) with prior estimates (B-F) of the transfer efficiency $T_{eff}(100 \rightarrow 1000)$ through the mesopelagic zone, defined as the ratio of POC flux at 1000 m to that at 100 m. Annotations in each panel show the mean transfer efficiency (calculated as the spatial mean of all values) for each estimate.

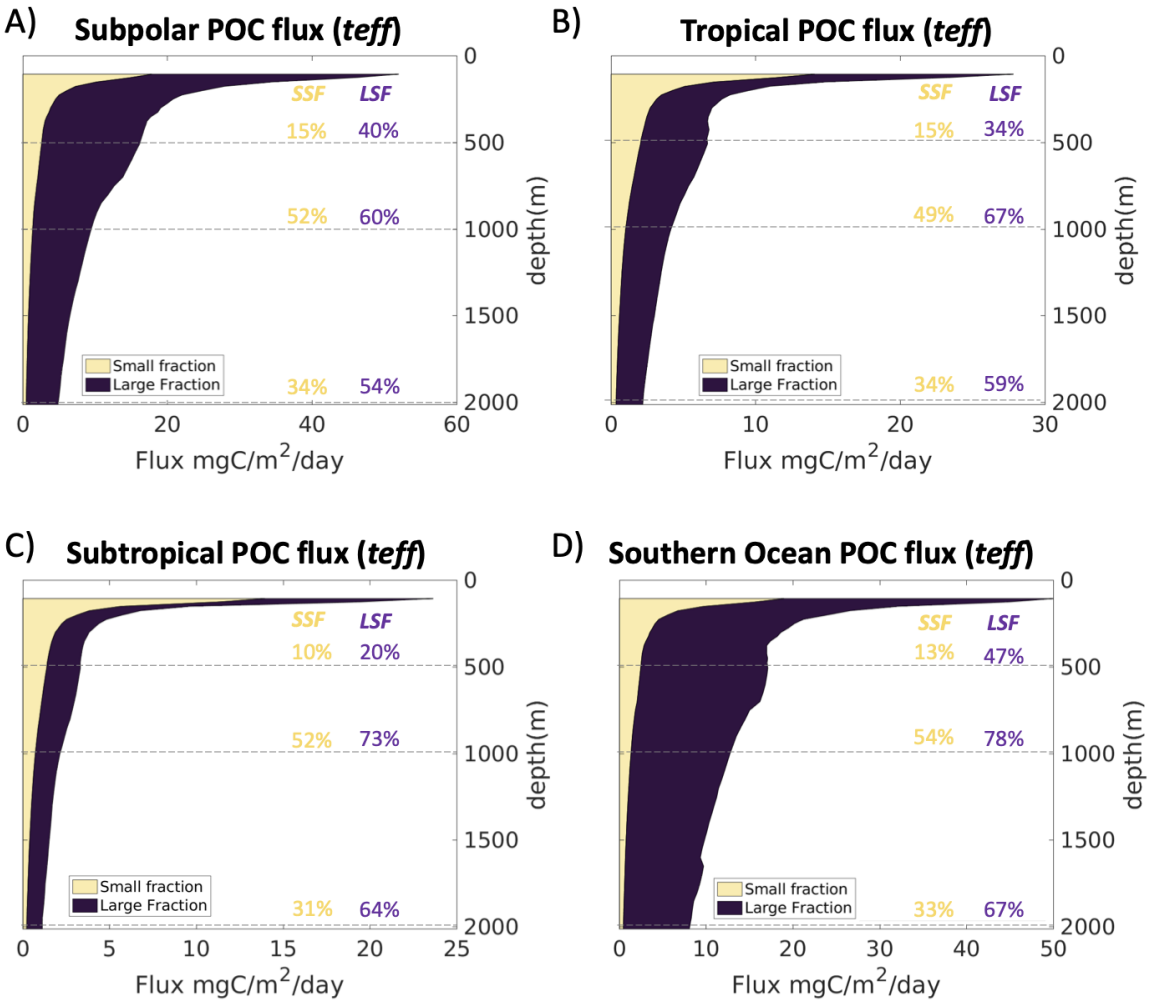


**Figure 9.** The size dependent flux through key ocean regions for the small size fraction (SSF; 35 $\mu$m - 418 $\mu$m) and the large size fraction (LSF; 418 $\mu$m - 5 mm). Annotations in each panel show transfer efficiencies though different layers, calculated as the ratio of the export at the deeper horizon to that at the shallow horizon bounding each layer, also separated by size.

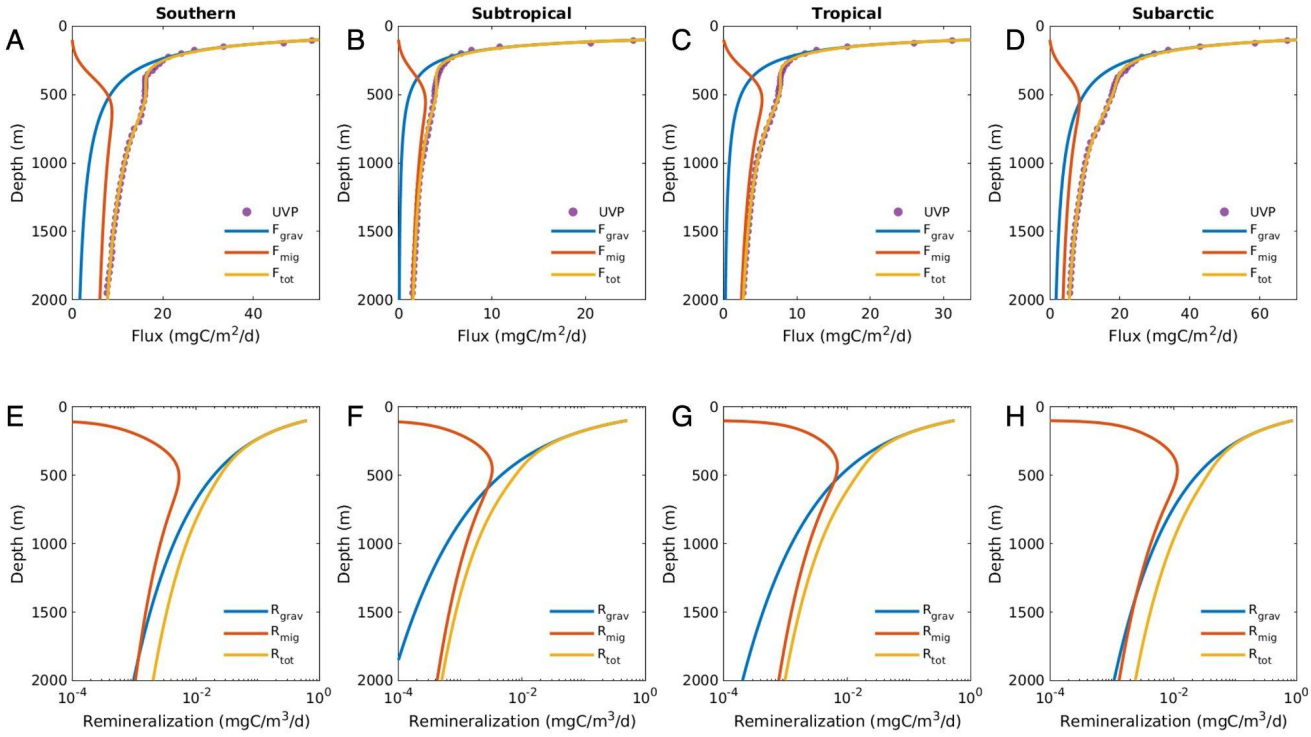


**Figure 10.** (A-D) Two-component flux model fit to the regional UVP5-based reconstructions, and separated into gravitational and migrant components. (E-H) The resulting remineralization rates (R) for each biological pump component.

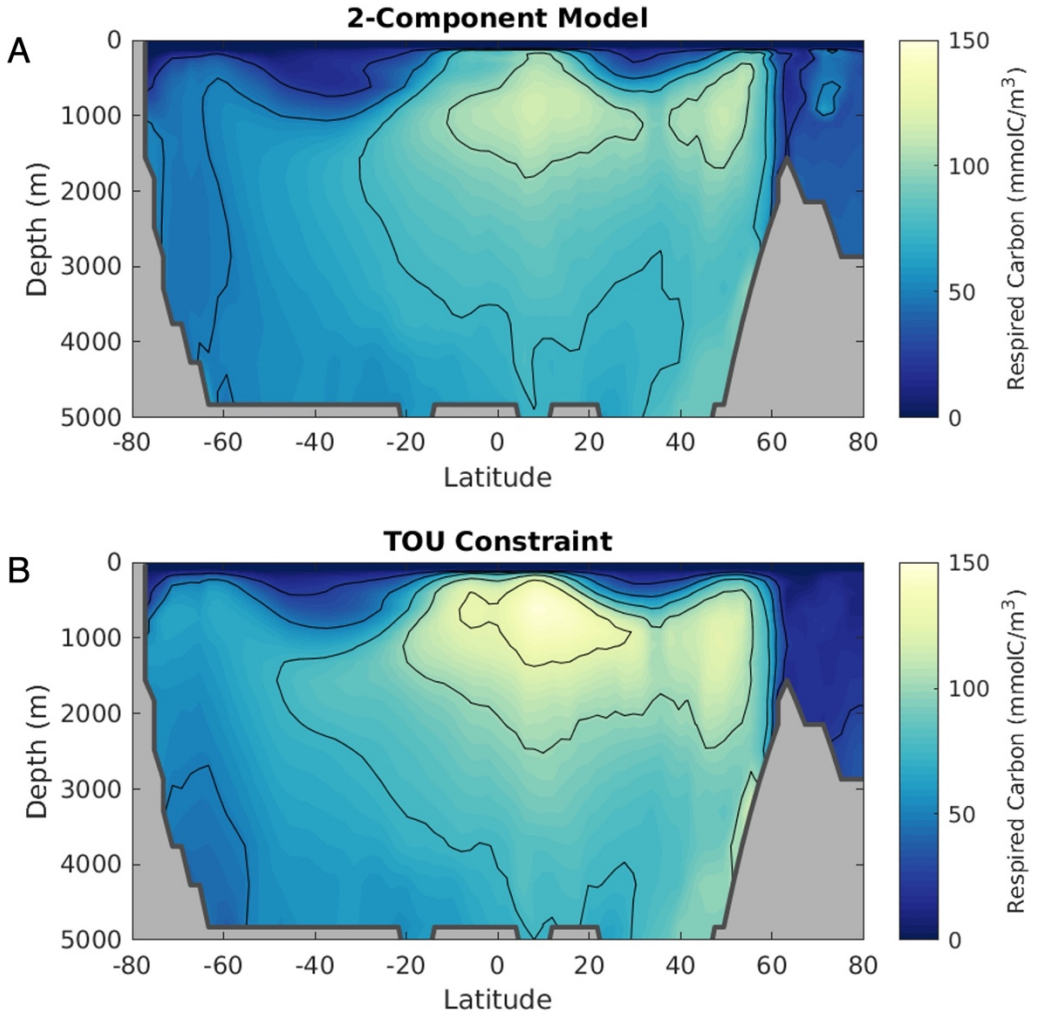


**Figure 11.** (A) Total respired carbon distribution predicted by our two-component model (i.e., the sum for Fig. 4D and 4E). (B) An observation-based estimate of the respired carbon distribution, generated by stoichiometrically converting total oxygen utilization (TOU) to carbon units (see Methods). We note that this constraint also includes the signature of other biological pump components (e.g. dissolved organic matter remineralization, respiration of fauna) so has a larger magnitude than the estimates based on POC remineralization alone (A).

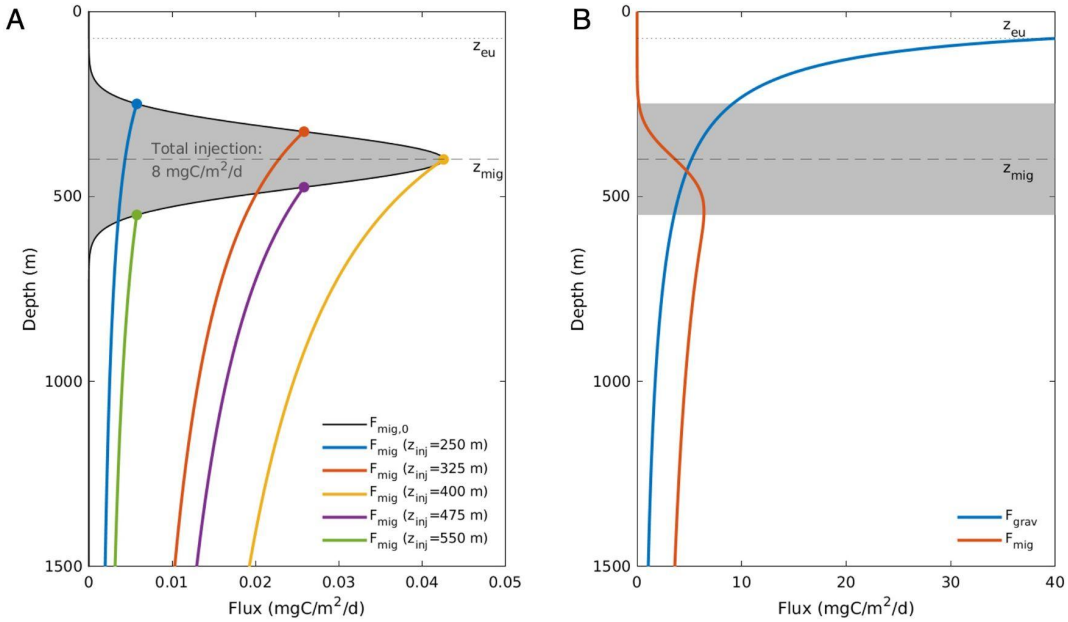


**Figure 12.** Demonstration of construction of the migrant-sourced particle flux in the two-component flux model for scenario with parameters $F_{grav,0}$ = 40 mg C $m^{-2}$ $d^{-1}$, $R_{mig}$ = 0.2, $Z_{mig}$ = 400m, $H_{mig}$ = 75m, $b_{grav}$ = 1.2, $b_{mig}$ = 0.6. (A) Particle injection rate by migrating organisms as a function of depth (shaded grey area, which integrates to $R_{mig}$ $F_{grav,0}$ = 8 mg $m^{-2}$ $d^{-1}$), and individual power-law flux profiles for particles injected at a range of different depths. (B) The total migrant-sourced flux ($F_{mig}$) is the sum of the individual flux profiles originating at every migration depth. It reaches its maximum flux towards the base of the migrant injection feature (grey shading represents $Z_{mig}$ +/- $2H_{mig}$), whereas the flux component exported gravitationally from the euphotic zone ($F_{grav}$) reaches its maximum flux at $z_{eu}$.